Frequency Clustering in Spontaneous Otoacoustic Emissions from a Lizard's Ear

Andrej Vilfan* and Thomas Duke[†]

*J. Stefan Institute, Ljubljana, Slovenia; and [†]London Center for Nanotechnology and Department of Physics & Astronomy, London, United Kingdom

ABSTRACT   Spontaneous otoacoustic emissions (SOAEs) are indicators of an active process in the inner ear that enhances the sensitivity and frequency selectivity of hearing. They are particularly regular and robust in certain lizards, so these animals are good model organisms for studying how SOAEs are generated. We show that the published properties of SOAEs in the bobtail lizard are wholly consistent with a mathematical model in which active oscillators, with exponentially varying characteristic frequencies, are coupled together in a chain by visco-elastic elements. Physically, each oscillator corresponds to a small group of hair cells, covered by a tectorial sallet, so our theoretical analysis directly links SOAEs to the micromechanics of active hair bundles.

INTRODUCTION

Spontaneous otoacoustic emissions (SOAEs) provide the most direct evidence of an active process in the inner ear, which is believed to aid the detection of low-level sounds by mechanically amplifying the incoming oscillatory stimuli. First detected in humans (1), they have also been recorded in a wide range of terrestrial vertebrates including other mammals (2), birds (3), frogs (4), and lizards (5). A similar phenomenon has been reported in some insects, such as the mosquito (6) and fruit fly (7), where the sensory antennae have been observed to vibrate at well-defined frequencies.

Because the properties of SOAEs are readily measured, they provide a convenient way of probing the active process without causing damage to the cochlea. Indeed, it is now routine to use the related transiently evoked otoacoustic emissions—emissions that are generated in response to a stimulus—to test the hearing of newborn infants (8). If we understood how the properties of SOAEs are determined, the study of their spectra and the way that frequency peaks shift in response to external stimuli would shed light on the underlying active process. In nonmammalian vertebrates, a great deal of evidence indicates that active amplification is intimately related to the sensory hair cells. In particular, in vitro experiments have shown that the stereovillar bundles of hair cells in the bullfrog sacculus oscillate spontaneously, and that this results in the addition of self-generated energy to signals at the corresponding frequency (9). Subsequently, an in vivo study of the modulation pattern of otoacoustic emissions generated by electrical stimulation of the inner ear of a lizard also implicated the stereovillar bundles as the source of the active process (10).

Lizards are particularly good model organisms for investigating SOAEs. Some species, including the bobtail lizard *Tiliqua rugosa* (5) and the Tokay gecko *Gekko gecko* (11,12), display a distinct spectrum of SOAEs with ~10 sharp, roughly equidistant frequency peaks, that can be suppressed and to a certain extent shifted by external tones (13). These emissions are thought to be generated in a region of the basilar papilla where the hair cells are covered by a tectorial membrane that is not continuous, but subdivided into sallets. In the gecko, this corresponds to the postaxial area of the apical (high frequency) segment (14) and in the bobtail lizard to the basal (high frequency) segment (15). The size of a sallet, the number of hair bundles attached to it, as well as the height of the bundles and the number of stereocilia they contain, vary with the position on the papilla, from the basal to the apical end (15,16).

The fact that the number of peaks in the SOAE spectrum is much smaller (by a factor of 8 in the bobtail lizard and smaller still in the Tokay gecko) than the number of sallets suggests that the peaks might result from coupled oscillations of a group of neighboring sallets, as originally suggested by Köppl and Manley (5), following the model assumptions of Manley et al. (16,17). In this article, we construct a theoretical model to test this hypothesis. Because of the amount of experimental data available (5,10,13,18–20), we use the properties of the bobtail lizard papilla in the quantitative aspects of our model. In the basal segment of this papilla, the tectorial membrane is subdivided into ~80 sallets, connected by a ropelike interconnection in the middle (15). Each sallet is attached to ~10–25 hair cells.

A previous theoretical model for the similar papilla of *Gekko gecko* (21) describes it as a chain of passive oscillators and describes its mechanical properties in great detail. This model can reproduce the resonant response of sallets, but, lacking an active mechanism, it is not intended to reproduce the spontaneous otoacoustic emissions. Models of active coupled oscillators, on the other hand, have been proposed

previously for the mammalian cochlea (22) and a related model produces a nonuniform otoacoustic emission spectrum, due to entrainment and suppression of oscillations (23). The mechanism is similar to the one we discuss here, although the physical basis of our model is quite different, due to the nature of sallets and the coupling between them.

Many of the properties of SOAEs that we describe with our model have also been observed in other lizard species that lack the tectorial structure (24). In this case, coupling between hair cells is likely to be hydrodynamic. While an appropriate model for this situation would have many similarities with the one discussed here, the long-range nature of the interactions would make it more complex. We therefore choose to concentrate on lizards with sallets, for which the physical situation is much better known.

THE MODEL

Our basic premise is that each of the hair bundles in the papilla is an active mechanical system that can generate self-sustained oscillations at a characteristic frequency. Moreover, we suppose that each hair bundle has a feedback control system that maintains it on the verge of its oscillatory instability (25,26). Then each of the sallets will vibrate with a small amplitude of displacement, driven by the dynamics of the hair cells that lie beneath it. We assume that, in the absence of any connection between the sallets, each sallet would vibrate at a different frequency, varying monotonically along the papilla, as a consequence of the changing architecture. However, the ropelike connection between the sallets will cause the dynamics of neighboring sallets to become coupled and might result in collective oscillatory dynamics.

Based on this premise, we introduce a model of N active oscillators, coupled through elastic (reactive) and viscous (dissipative) elements. Each oscillator describes one sallet and its connected hair bundles. We choose $N = 80$, corresponding to the number of sallets in the bobtail lizard (15). It has been shown before that, unlike in freestanding hair bundles, inertia is important in determining the characteristic frequency of a sallet (21). Each oscillator is therefore described by the equation of motion,

$$M_j\ddot{x}_j = -K_j x_j - \Gamma_j \dot{x}_j + O(x^3) + F_j + \zeta_j, \quad (1)$$

where M_j is the mass of jth oscillator, K_j is its spring constant, and Γ_j is the effective damping (which can be negative for an active oscillator). $O(x^3)$ denotes cubic terms that describe the nonlinearity, which is inevitable in an active oscillator and determines the amplitude of spontaneous oscillations. F_j represents the force exerted on a sallet by its neighbors and reads

$$F_j = k(x_{j+1} - x_j) + k(x_{j-1} - x_j) \\ + \gamma(\dot{x}_{j+1} - \dot{x}_j) + \gamma(\dot{x}_{j-1} - \dot{x}_j), \quad (2)$$

for sallets that are not at the ends of the chain (Fig. 1). Here k represents the reactive nearest-neighbor coupling (corresponding to elastic elements that connect the oscillators) and γ the dissipative coupling (corresponding to viscous damping of the relative motion between neighboring oscillators).

In addition, each sallet is subject to noise. We assume that the major source of noise is thermal, from the Brownian motion of the surrounding fluid, and neglect the contributions of the dissipative coupling between the sallets (γ) and of the active driving mechanism within the hair bundles. Then according to the fluctuation-dissipation theorem, the magnitude of the noise is related to the corresponding friction coefficient Γ_F and the Brownian force on each sallet is given by

$$\langle \zeta_j(t)\zeta_j(0)\rangle = 2\Gamma_F k_B T \delta(t). \quad (3)$$

We first rewrite Eq. 1 using the complex notation

$$z_j = x_j - \frac{1}{\omega_j} i\dot{x}_j, \quad (4)$$

giving

$$\dot{z}_j = i\omega_j z_j + 2\varepsilon_j i \operatorname{Im} z_j + 2id_I \operatorname{Re}(z_{j+1} + z_{j-1} - 2z_j) \\ + 2id_R \operatorname{Im}(z_{j+1} + z_{j-1} - 2z_j) + i\tilde{\zeta}_j(t) + O(z^3) \quad (5)$$

where

$$\omega_j = \sqrt{\frac{K_j}{M_j}}, \quad (6)$$

$$\varepsilon_j = -\frac{\Gamma_j}{2M_j}, \quad (7)$$

$$d_I = -\frac{1}{2}\frac{k}{\sqrt{K_j M_j}}, \quad (8)$$

$$d_R = \frac{1}{2}\frac{\gamma}{M_j}, \quad (9)$$

$$\tilde{\zeta}_j(t) = \frac{\zeta_j(t)}{M_j \omega_j}. \quad (10)$$

Equation 5 for each oscillator can be transformed to the normal form of a Hopf bifurcation (27). If the system is close to the bifurcation ($\varepsilon_j \ll \omega_j$) and the amplitudes are small, this transformation simply means that all terms containing $\bar{z}$, $\bar{z}^3$, $z\bar{z}^2$, and z^3 can be neglected. Equation 5 then simplifies to
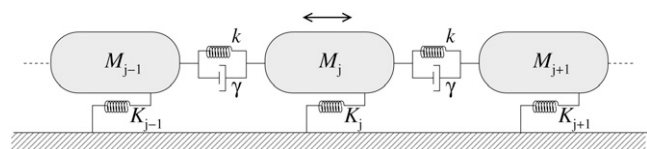

FIGURE 1 Mechanical equivalent of the model. Sallets are represented as inertial oscillators (mass M_j, spring K_j), coupled to their neighbors by elastic (constant k) and damping (constant γ) elements. In addition, there exists an active driving mechanism within each oscillator (not shown).

$$\dot{z}_j = (i\omega_j + \varepsilon_j)z_j + (d_R + id_I)(z_{j+1} + z_{j-1} - 2z_j)$$
$$+ \tilde{\zeta}_j(t) - B|z_j|^2 z_j. \quad (11)$$

Naturally, the second term differs for the oscillators at the ends of the chain; it should be replaced by $(d_R + id_I)(z_2 - z_1)$ for $j = 1$ and by $(d_R + id_I)(z_{N-1} - z_N)$ for $j = N$. The coefficient B describes the intrinsic nonlinearity of the oscillators and is necessary to preserve a finite amplitude. Equation 11 is a type of complex Ginzburg-Landau lattice equation (28–30) with a nonuniform distribution of characteristic frequencies ω_j. It displays two symmetries: under the transformation $\omega_j \rightarrow \omega_j + const$ while preserving d_I; and under the transformation $\omega_j \rightarrow const - \omega_j$, with $d_I \rightarrow -d_I$. The first symmetry means that the properties of the model only depend on characteristic frequency differences between oscillators, but not on their absolute values. The second means that we do not lose any generality by discussing the model with a negative d_I; a positive value would lead to the same effects with a reversed frequency range. As one can see, elastic springs between sallets result in a complex coupling constant $d = d_R + id_I$ (also called nonscalar coupling). Purely dissipative connections, on the other hand, result in a real (i.e., scalar) coupling constant d.

RESULTS

Model system: regular and noiseless

It is instructive to start our analysis by investigating the solutions of Eq. 11 in the absence of noise ($\tilde{\zeta}_j = 0$), and for a regular system in which the characteristic frequencies vary linearly along the chain, $\omega_j = \omega_1 + (j - 1)\Delta\omega$. To provide a wide range of frequencies, we choose $\Delta\omega$ such that $\omega_N/\omega_1 = 5$. Because we have scant information about the physical nature of the coupling between the oscillators, we consider the simplest situation in which the coupling constants d_R and d_I do not vary with position. Further, we suppose that each of the oscillators is close to its Hopf bifurcation, such that $\varepsilon_j = \varepsilon$ for all j, where ε is a small positive number.

In general, we find that the oscillators entrain one another such that the chain splits up into a number of clusters. The group of oscillators within a cluster all vibrate at the same frequency, and the frequency shifts abruptly from one cluster to the next. The precise way that this clustering occurs, however, depends on whether the coupling is dissipative or reactive.

Clustering with dissipative coupling

The system with a real coupling parameter has been studied previously, initially using phase oscillators (31) and subsequently using Ginzburg-Landau oscillators (32). The two models do not behave identically: the frequency plateaus observed in the Ginzburg-Landau model (32) are more regular and equidistant than those seen in weakly coupled phase oscillators (31).

An example of the time-averaged frequencies and amplitudes of the oscillators in a dissipatively-coupled chain is shown in Fig. 2 A. The oscillators synchronize themselves within clusters, with each cluster containing $N_n \approx \sqrt{8d_R/\Delta\omega}$ oscillators (32). This behavior is apparent in Fig. 2 A, where a smaller value of $\Delta\omega$ permits a larger number of oscillators to synchronize with one another, and also reduces the size of the jump between frequency plateaus. The ordered structure of the frequency plateaus is symmetric with respect to the direction along the chain, and each cluster oscillates at a frequency close to the average characteristic frequency of the oscillators that it contains.

We note that the coupling constant needs to be relatively strong to split the chain into just a few clusters, as illustrated
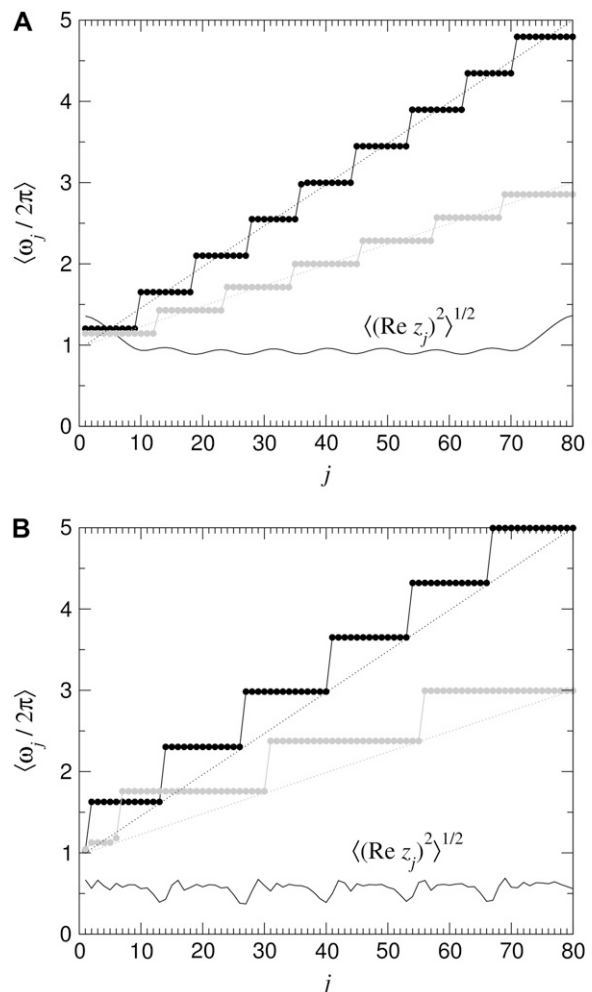

FIGURE 2 (A) Average frequency $\langle \omega_j/2\pi \rangle$ (line with circles) and amplitude $\sqrt{\langle (\mathrm{Re}\, z_j)^2 \rangle}$ (continuous line) of each oscillator in a dissipatively coupled chain. The dashed line shows the characteristic frequency $\omega_j/2\pi$ of each oscillator. The parameters are $\omega_1 = 2\pi$, $\omega_N = 5 \times 2\pi$ (solid), $\omega_N = 3 \times 2\pi$ (shaded), $N = 80$, $d_R = 16$, $d_I = 0$, $\varepsilon = 4$, and $B = 1$. (B) Results for a chain with complex coupling. The parameters are $\omega_1 = 2\pi$, $\omega_N = 5 \times 2\pi$ (solid), $\omega_N = 3 \times 2\pi$ (shaded), $N = 80$, $\varepsilon = 1.0$, $d_R = 0.15$, $d_I = -1.0$, and $B = 1$. Clearly visible is the entrainment of the chain from high toward low frequencies.

in Fig. 2 A where $d_R = 2.5\omega_1$. Such strong coupling tends to lead to ''oscillator death'' (32), i.e., it kills the active vibration of individual oscillators, and so the value of the control parameter ε has to be increased to compensate. As a result, the oscillators are quite far from their Hopf bifurcation, and we might expect this to impact on their sensitivity and dynamic range. For this reason, dissipative coupling appears to be less than ideal.

Clustering with reactive coupling

If the oscillators are coupled with elastic elements only, one can see from Eqs. 8 and 9 that the coupling constant d is purely imaginary and that the imaginary part has a negative sign, i.e., $d_R = 0$, $d_I < 0$. This reactive coupling can lead to very complex behavior, even when just two oscillators are connected together (33). Chains of reactively coupled phase oscillators have been studied in Rosenau and Pikovsky (29), where they have been shown to have various different modes of perturbations that can propagate along the chain.

One distinct feature of reactive coupling can be illustrated in a system containing two oscillators. Suppose oscillator 1 is forced to oscillate with a certain amplitude at its natural frequency ω_1. The motion of the oscillator 2, coupled to it, is described by

$$\dot{z}_2 = (i\omega_2 + \varepsilon_2)z_2 + (d_R + id_I)(z_1 - z_2) - B|z_2|^2 z_2. \quad (12)$$

If we further assume that oscillator 2 can be treated like a phase oscillator, ($|z_2| = const$), we obtain the equation of motion for its phase

$$\dot{\phi}_2 = \omega_2 + d_R \sin(\phi_1 - \phi_2) + d_I(\cos(\phi_1 - \phi_2) - 1). \quad (13)$$

With $d_R = 0$ and $d_I < 0$, one can see that the oscillator 2 can only be entrained to the frequency ω_1 if $\omega_2 < \omega_1 < \omega_2 - 2d_I$, i.e., the entrainment frequency must lie in an interval above the characteristic frequency ω_2 of oscillator 2.

This feature pertains in a chain of oscillators. Each oscillator can be entrained by motion at a frequency higher than its characteristic frequency, but not by motion at a lower frequency. Therefore, in a chain of oscillators, the order spreads from high to low frequencies. This can be seen clearly in the example shown in Fig. 2 B. The oscillator at the end of the chain with the highest characteristic frequency, ω_N, oscillates at that frequency and entrains its near neighbors to form a synchronized cluster. At some distance along the chain, an oscillator with a lower characteristic frequency is unable to keep pace; it therefore oscillates at its characteristic frequency and, in turn, entrains its near neighbors to make a second cluster; and so on down the chain.

Note that the symmetry of Eq. 11 mentioned above implies that the directionality of entrainment is reversed if $d_I > 0$, in which case order would spread from low to high frequencies. The quantity $d_I > 0$ corresponds to negative elasticity in connections ($k < 0$), so such behavior would be unusual.

Emission spectrum and response to external tones

We determine the emission spectrum as the power spectrum $S(\omega)$ of the summed displacement X of the oscillators

$$X = \sum_{j=1}^{N} x_j = \text{Re} \sum_{j=1}^{N} z_j, \quad (14)$$

$$S(\omega) = \frac{1}{T}\left| \int_0^T X(t)\, e^{i\omega t} dt \right|^2. \quad (15)$$

The spectrum (Fig. 3) clearly shows distinct peaks at the frequency plateau values.

Of experimental, as well as theoretical, importance is the response of the system to an external tone. We model a tone
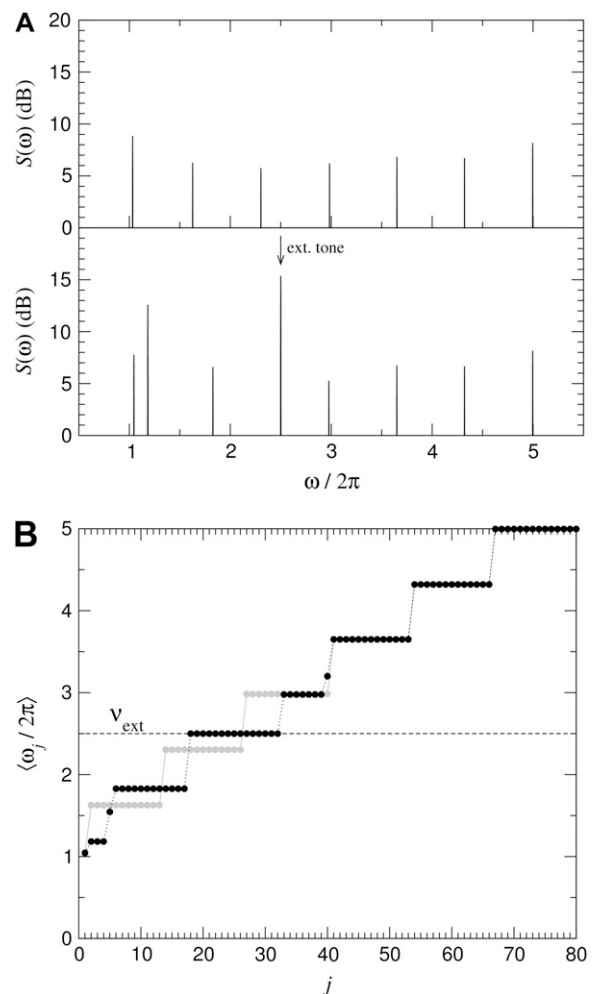

FIGURE 3 (A) Emission spectrum as defined by Eq. 15 for the system with parameters $\varepsilon = 1.0$, $d_R = 0.15$, $d_I = -1.0$, $N = 80$, $\omega_1 = 1 \times 2\pi$, $\omega_N = 5 \times 2\pi$, and $B = 1$. The top graph shows the unperturbed system and the bottom graph the system in the presence of an external tone with amplitude $F_{ext} = 1.0$ and frequency $\nu_{ext} = 2.5$. (B) Average frequency of oscillation for each oscillator in the same system (shaded, unperturbed and solid, with an external tone). The external tone mainly changes emission peaks and frequency plateaus below its own frequency.

as a sinusoidal force that acts on all oscillators in the same way:

$$\bar{F}_j(t) = F_{ext}\cos(\omega_{ext}t). \tag{16}$$

If the external force is sufficiently large, it entrains a number of oscillators (those with sufficiently close characteristic frequencies) to its own frequency. For the reasons described above, when the coupling is reactive the oscillators whose characteristic frequency significantly exceeds the tone frequency are unaffected, while the oscillators with lower characteristic frequency reorganize into a different set of synchronized clusters. This is reflected in the emission spectrum: for $\omega \gg \omega_{ext}$, the spectrum is largely unaffected; for $\omega \gtrsim \omega_{ext}$, the peaks are suppressed but they hardly shift in frequency; and for $\omega < \omega_{ext}$, the peaks shift in frequency but are not suppressed.

Exponential frequency distribution

Measurements of characteristic frequencies of nerve fibers in bobtail lizard indicate that these frequencies vary approximately exponentially with the position on the papilla (34). We therefore use the distribution

$$\omega_j = \omega_1 \left(\frac{\omega_N}{\omega_1}\right)^{\frac{j-1}{N-1}}. \tag{17}$$

The resulting average frequencies are shown in Fig. 4. Note that the even spacing of the frequency plateaus is largely unaffected by the exponential variation of characteristic frequencies; rather, it is the number of oscillators per cluster that adjusts to maintain an approximately uniform spacing of cluster frequencies.
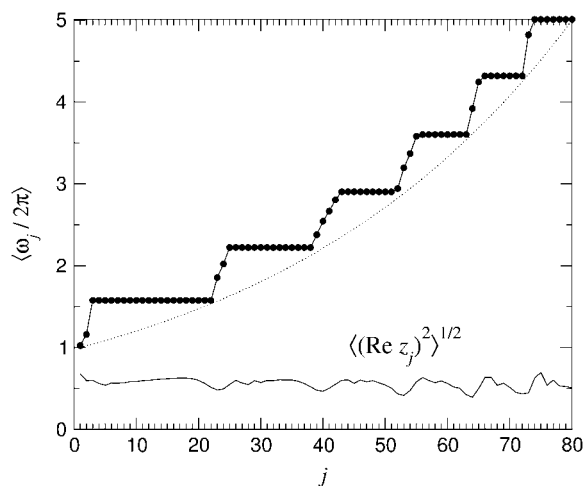

FIGURE 4 Average frequency of each oscillator (*line* with *circles*) in a chain with an exponential distribution of characteristic frequencies ω_j (*dotted line*). All other parameters correspond to those in Fig. 2 *B*.

Realistic system: disordered and noisy

Experimentally measured spectra of SOAEs from lizards' ears do not display the regularity and the sharpness of the peaks seen in the model system discussed in the previous section. To construct a more realistic mathematical model of SOAE generation, we shall use the exponential frequency distribution, given by Eq. 17, and make the following modifications:

1. Physical irregularities. Because the spatial patterning of the papilla is imperfect, we assume that the actual characteristic frequencies ω_j deviate by $\pm 1\%$ from the value given by Eq. 17. Likewise, we assume a $\pm 20\%$ randomness in the control parameter ε_j and in the coupling constants d_R and d_I between each pair of oscillators. These irregularities are assumed to be fixed and not to vary with time. A higher level of variations would make the peaks less regular, but more stable against external tones.

2. Thermal noise. We include a stochastic force $\tilde{\zeta}_j(t)$, which has the autocorrelation function

$$\langle \tilde{\zeta}_j(t + \tau)\tilde{\zeta}_j(t)\rangle = 2\bar{D}\delta(\tau). \tag{18}$$

An estimate for the amplitude of the noise term, using the Einstein relation, is given in the Appendix.

While we know the number of oscillators N and their characteristic frequencies ω_j, other parameters are more difficult to determine. We have chosen values of d_R and d_I to reproduce a realistic number of peaks in the spectrum (~ 10 in total). We know little about the control parameter ε except that its value should be sufficiently smaller than ω if the oscillators are to operate in the vicinity of a Hopf bifurcation, where they have the greatest sensitivity (25). We therefore choose a value that is an order-of-magnitude smaller than the lowest characteristic frequency ω_1. The absolute value of the nonlinear coefficient B is not important, because it only determines the amplitude z of oscillation and does not affect the properties of the model in a qualitative fashion.

Emission spectrum and response to external tones

The clustering of the oscillators in this realistic model, and the corresponding emission spectrum, are shown in Fig. 5. The main consequence of the disorder is that the locations of the frequency plateaus, and thus the frequencies of the peaks in the spectrum, are not determined exclusively by ordering from the high frequency end; instead, they tend to be pinned to a few preferred values where the local realization of the disorder favors synchronization.

The spectra reproduce well those observed in Köppl and Manley (5). Some discrepancy can be seen with regard to the width of emission peaks and the baseline emission between peaks. The latter is not fully comparable, because the cal-
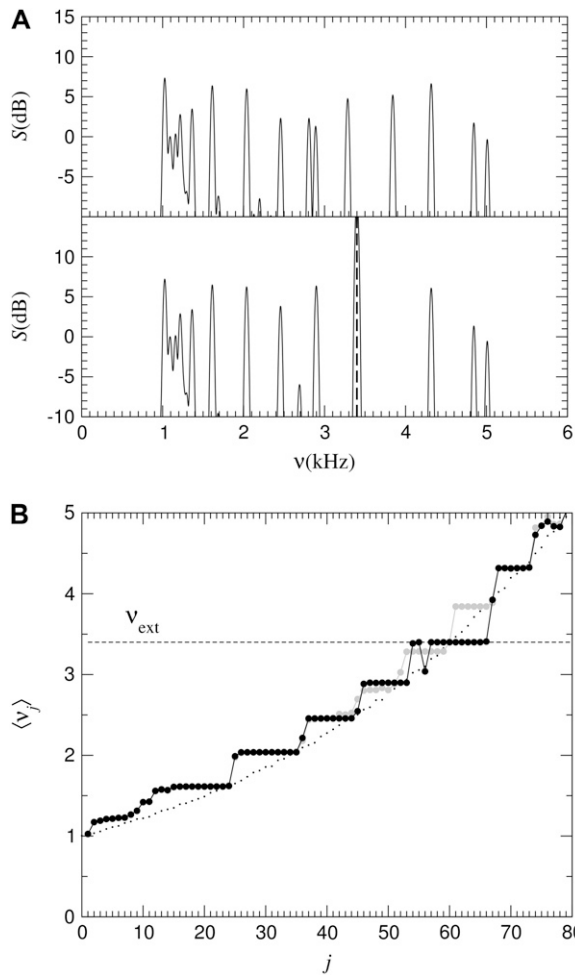
FIGURE 5 (*A*) Emission spectrum for the disordered system in the absence (*top*) and presence (*bottom*) of an external tone with a frequency of $\nu_{ext} = 3.4$ kHz. Parameters: $\varepsilon = 628$ s^{-1}, $d_R = 157$ s^{-1}, $d_I = -754$ s^{-1}, $2\bar{D} = 0.157$ s^{-1}, and $B = 6280$ s^{-1}. A Gaussian filter ($\sigma = 15$ Hz) is applied to the spectra. (*B*) Average frequency of each oscillator in the absence (*shaded*) and in the presence (*solid*) of the same external tone. The dotted line shows the characteristic frequencies of individual oscillators.

culated spectra only contain the indirect influence of noise acting on sallets, but not direct noise sources. A possible explanation for the wider peaks is that the characteristic frequencies are not entirely stable on the timescale at which the spectra are recorded. Alternatively, the noise amplitude calculated in the previous section may be an underestimate.

When an external tone is applied, the oscillators whose characteristic frequencies are close to the tone frequency are entrained by the stimulus. As a result, the emission peaks closest to the tone frequency vanish, while some of the other peaks shift in frequency. The shifts are particularly strong for peaks with frequencies below that of the external tone, reflecting our earlier observation that the oscillators are entrained from the high frequency end of each cluster. The results reproduce the behavior seen in Köppl and Manley (13).

The effect of an external tone with a given frequency on an emission peak with a different frequency is best represented by an amplitude input/output function. This measures the amplitude of the emission peak (whether or not it has shifted in frequency) as a function of the external tone amplitude. A typical example is shown in Fig. 6 *A*. For strong stimuli, the I/O function invariably exhibits a steep decline. This reflects the fact that the oscillators that form a synchronized cluster in the absence of the tone (and thereby generate the spontaneous emission) get entrained by a stimulus (so that the emission is diminished, or disappears). The I/O function of some emission peaks shows a remarkable feature: in an intermediate range of amplitudes of the external tone, the stimulus can actually augment the amplitude of the emission
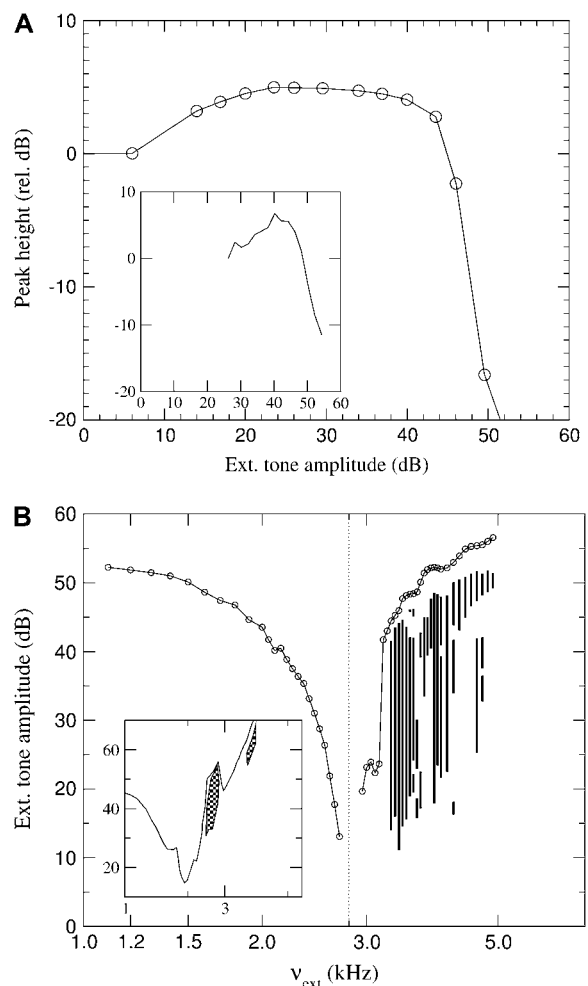

FIGURE 6 (*A*) Amplitude input/output function for the peak at 2.8 kHz in response to an external tone at 3.4 kHz. This I/O function shows the phenomenon of facilitation: the amplitude of the emission peak is augmented for moderate amplitudes of the external tone. (*B*) Iso-suppression function of the peak at 2.8 kHz. The circles show for each frequency ν_{ext} the amplitude of the external tone that is necessary to suppress the emission peak at 2.8 kHz by 2 dB. The hatched field shows the region where the emission is facilitated (augmented) by at least 2 dB. Both insets show comparable experimental data from Köppl and Manley (13).

(see Fig. 6 *A*). This phenomenon has been reported experimentally and is known as ''facilitation'' (13). The explanation of this effect is best understood by reference to Fig. 5 *B*, and by examining the oscillators that spontaneously form the synchronized cluster with a frequency slightly lower than the frequency of the external tone. A stimulus of moderate amplitude entrains many, but not all of these oscillators. As a result, the cluster breaks up and some of the oscillators join the adjacent cluster at lower frequency, increasing its size. Thus, the amplitude of the corresponding emission peak is enhanced. We find that facilitation is mostly limited to situations where the external tone has a higher frequency than the emission peak. Its exact shape depends on the peak chosen and on the particular representation of the random disorder in frequencies and control parameters.

Another way of presenting the effect of an external tone on an emission peak is to plot the iso-suppression curve. This shows, as a function of the external tone frequency, the amplitude that is needed to suppress a given peak by 2dB (Fig. 6 *B*). Likewise, one can determine the regions of facilitation, where the peak is augmented by at least 2dB (*hatched area* in the *graph*). The results of the model correspond quite closely to experimental observations (13). As reported for emissions from the bobtail lizard, the facilitation windows are typically restricted to the right side of the graph, where the external tone frequency is higher than the emission frequency, although we observe facilitation over a more extensive range of amplitudes than is seen experimentally. The redistribution of oscillators among synchronized clusters of sallets may be only a partial explanation of facilitation, for the phenomenon has also been observed in species that have a continuous tectorial membrane (35) and in species that have no tectorial membrane (24).

Sensitivity of a coupled chain of active oscillators

The close correspondence between the behavior of our model system and the experimental data on emissions from the bobtail lizard strongly support the hypothesis that the emissions result from the reactive coupling of a chain of active oscillators. One question that arises is whether this arrangement confers any advantages that improve the performance of the cochlea in its principal function—the detection of sound. To explore this issue we compare the realistic model system of coupled oscillators, described in the previous section, with a system of similar oscillators with minimal coupling, consisting only of the dissipative part d_R. We use two criteria to evaluate the potential sensitivity of such a system: the relative amplitude response and the degree of phase locking. These quantities directly determine the postsynaptic firing rate and the regularity of spike timings in the auditory nerve, as measured experimentally (36,37). While the firing rate is thought to be used to differentiate different levels of sound at moderate and high intensities, phase

locking allows for a more sensitive way of detecting low intensity sound.

We define the amplitude response as

$$R_j = \frac{\sqrt{\langle (\mathrm{Re}\, z_{j(F)})^2 \rangle}}{\sqrt{\langle (\mathrm{Re}\, z_{j(0)})^2 \rangle}}, \qquad (19)$$

where $z_{j(F)}$ represents the complex variable of the oscillator j in the presence of the external force and $z_{j(0)}$ in the unperturbed system.

A measure for the degree of phase locking is the absolute vector size, defined as

$$v_j = \sqrt{\langle \sin(\phi_j - \phi_0)\rangle^2 + \langle \cos(\phi_j - \phi_0)\rangle^2}, \qquad (20)$$

where ϕ_j is the phase of z_j and $\phi_0 = \omega_{ext} t$ is the phase of the external tone. Angle brackets denote time-averaging. Note that the maximum response occurs in oscillators whose characteristic frequency is somewhat below the tone frequency, which is a property of the chain with reactive coupling.

A comparison of both quantities for the realistic system with full coupling and the system without a reactive coupling component is shown in Fig. 7. This comparison could shed some light on the benefits conferred by elastic connections between sallets, while dissipative coupling is inevitable due to hydrodynamic effects. In the realistic system, the amplitude response is stronger but also much more scattered, with some oscillators increasing in amplitude while others decrease. More significantly, the degree of phase locking is
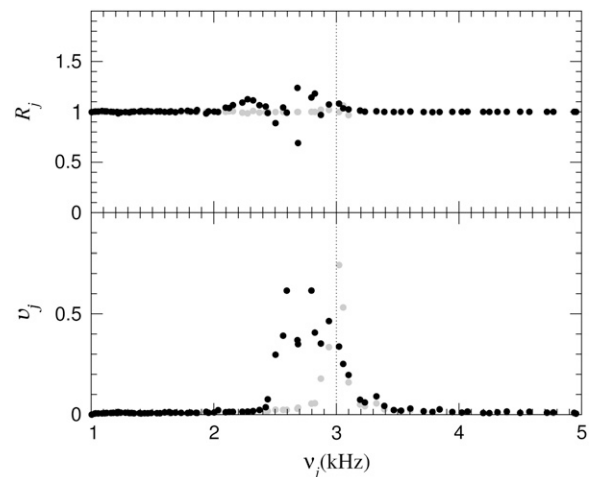

FIGURE 7 Comparison between the full model with reactive and dissipative coupling (*solid*, $d_R = 157\ \mathrm{s}^{-1}$, $d_I = -754\ \mathrm{s}^{-1}$) and a model with no reactive component in the coupling (*shaded*, $d_R = 157\ \mathrm{s}^{-1}$, $d_I = 0$). The top panel shows the relative amplitude response R_j of each sallet (as a function of its characteristic frequency ν_j) to an external tone with frequency 3 kHz. The bottom panel shows the degree of phase locking v_j of each sallet to the external tone. These response functions are similar throughout the spectrum, except for the fine structure of the irregularities.

substantial for a much larger number of oscillators in the realistic system. This suggests that reactive coupling may be beneficial for the detection of faint sounds.

SUMMARY

Our theoretical results provide compelling evidence that SOAEs in lizards are a by-product of the active micromechanics of hair bundles. By extension, it seems likely that SOAEs in other nonmammalian vertebrates originate in the active movement of hair bundles, and that the varying properties of emissions among species are a consequence of different physical coupling between hair cells. SOAE generation in the mammalian cochlea is considerably more complex, as a result of the propagating wave on the basilar membrane; in this case, the spectrum of emission modes most likely depends on constructive interference of waves, determined by properties of the cochlea as a whole (38). Because the performance of lizards' ears almost matches that of mammals, our results indicate that good hearing can be achieved by fairly simple means. All that is needed for sensitive, frequency-selective, and tonotopic audition is a coupled chain of grouped hair cells, incorporating an active process in their bundles that generates oscillations with characteristic frequencies that vary monotonically along the chain.

APPENDIX

In the following, we estimate the amplitude of the stochastic force in the noisy system. The amplitude of the physical noise in the real system is determined by the Einstein relation, Eq. 3. Using the transformation given by Eq. 10, the amplitude of the dimensionless noise term, $\tilde{\zeta}_j$, that appears in Eq. 11 is

$$\tilde{D}_j = \frac{\Gamma_F k_B T}{\left(M_j \omega_j\right)^2}. \tag{21}$$

For the sake of simplicity, we assume that the noise term has identical magnitude for all oscillators. The viscous friction coefficient Γ_F of a sallet can be estimated from its Q factor

$$\Gamma_F = \frac{M\omega}{Q}, \tag{22}$$

which leads to the expression

$$\tilde{D} = \frac{k_B T}{QM\omega}. \tag{23}$$

Finally, because we wish to know the magnitude of the noise term relative to the magnitude of spontaneous oscillations, we calculate the quantity $2\tilde{D}/A^2$. We estimate it by using the following values for a sallet with a frequency in the middle of the spectrum: $\omega = 2\pi \times 3000\ \text{s}^{-1}$, $M = 10^{-11}\ \text{kg}$ (16), $Q = 10$ (16), $A = 30\ \text{nm}$, and $k_B T = 4.1 \times 10^{-21}\ \text{J}$. We then obtain $2\tilde{D}/A^2 \approx 4.8\ \text{s}^{-1}$. In the simulation, the dimensionless amplitude was $\tilde{A} = \sqrt{\langle|z^2|\rangle} \approx 0.21$, and we therefore estimate the noise amplitude as $2\tilde{D} \approx 0.2\ \text{s}^{-1}$.

REFERENCES

1. Zurek, P. M. 1981. Spontaneous narrowband acoustic signals emitted by human ears. *J. Acoust. Soc. Am.* 69:514–523.

2. Zurek, P. M. 1985. Acoustic emissions from the ear: a summary of results from humans and animals. *J. Acoust. Soc. Am.* 78:340–344.

3. Taschenberger, G., and G. A. Manley. 1997. Spontaneous otoacoustic emissions in the barn owl. *Hear. Res.* 110:61–76.

4. van Dijk, P., P. M. Narins, and J. Wang. 1996. Spontaneous otoacoustic emissions in seven frog species. *Hear. Res.* 101:102–112.

5. Köppl, C., and G. A. Manley. 1993. Spontaneous otoacoustic emissions in the bobtail lizard. I: General characteristics. *Hear. Res.* 71:157–169.

6. Göpfert, M. C., and D. Robert. 2001. Active auditory mechanics in mosquitoes. *Proc. R. Soc. Lond. B. Biol. Sci.* 268:333–339.

7. Göpfert, M. C., and D. Robert. 2002. The mechanical basis of *Drosophila* audition. *J. Exp. Biol.* 205:1199–1208.

8. Kemp, D. 2002. Otoacoustic emissions, their origin in cochlear function, and use. *Br. Med. Bull.* 63:223–241.

9. Martin, P., and A. J. Hudspeth. 1999. Active hair-bundle movements can amplify a hair cell's response to oscillatory mechanical stimuli. *Proc. Natl. Acad. Sci. USA.* 96:14306–14311.

10. Manley, G. A., D. L. Kirk, C. Köppl, and G. K. Yates. 2001. In vivo evidence for a cochlear amplifier in the hair-cell bundle of lizards. *Proc. Natl. Acad. Sci. USA.* 98:2826–2831.

11. Manley, G. A., L. Gallo, and C. Köppl. 1996. Spontaneous otoacoustic emissions in two gecko species, *Gekko gecko* and *Eublepharis macularius*. *J. Acoust. Soc. Am.* 99:1588–1603.

12. Stewart, C. E., and A. J. Hudspeth. 2000. Effects of salicylates and aminoglycosides on spontaneous otoacoustic emissions in the Tokay gecko. *Proc. Natl. Acad. Sci. USA.* 97:454–459.

13. Köppl, C., and G. A. Manley. 1994. Spontaneous otoacoustic emissions in the bobtail lizard. II: Interactions with external tones. *Hear. Res.* 72:159–170.

14. Köppl, C., and S. Authier. 1995. Quantitative anatomical basis for a model of micromechanical frequency tuning in the Tokay gecko, Gekko gecko. *Hear. Res.* 82:14–25.

15. Köppl, C. 1988. Morphology of the basilar papilla of the bobtail lizard *Tiliqua rugosa. Hear. Res.* 35:209–228.

16. Manley, G. A., C. Köppl, and G. K. Yates. 1989. Micromechanical basis of high-frequency tuning in the bobtail lizard. *In* Cochlear Mechanics. J. P. Wilson and D. T. Kemp, editors. Plenum, New York.

17. Manley, G. A., G. K. Yates, and C. Köppl. 1988. Auditory peripheral tuning: evidence for a simple resonance phenomenon in the lizard *Tiliqua. Hear. Res.* 33:181–189.

18. Manley, G. A., and C. Köppl. 1994. Spontaneous otoacoustic emissions in the bobtail lizard. III: Temperature effects. *Hear. Res.* 72:171–180.

19. Manley, G. A., and D. L. Kirk. 2002. The influence of injected AC and DC currents on spontaneous otoacoustic emissions in the bobtail lizard. *J. Assoc. Res. Otolaryngol.* 3:200–208.

20. Manley, G. A., and D. L. Kirk. 2005. BAPTA induces frequency shifts in vivo of spontaneous otoacoustic emissions of the bobtail lizard. *Audiol. Neurootol.* 10:248–257.

21. Authier, S., and G. A. Manley. 1995. A model of frequency tuning in the basilar papilla of the Tokay gecko, *Gekko gecko. Hear. Res.* 82:1–13.

22. Long, G. R., A. Tubis, and K. L. Jones. 1991. Modeling synchronization and suppression of spontaneous otoacoustic emissions using Van der Pol oscillators: effects of aspirin administration. *J. Acoust. Soc. Am.* 89:1201–1212.

23. van Hengel, P. W., H. Duifhuis, and M. P. van den Raadt. 1996. Spatial periodicity in the cochlea: the result of interaction of spontaneous emissions? *J. Acoust. Soc. Am.* 99:3566–3571.

24. Manley, G. A. 2006. Spontaneous otoacoustic emissions from free-standing stereovillar bundles of ten species of lizard with small papillae. *Hear. Res.* 212:33–47.

25. Camalet, S., T. Duke, F. Jülicher, and J. Prost. 2000. Auditory sensitivity provided by self-tuned critical oscillations of hair cells. *Proc. Natl. Acad. Sci. USA.* 97:3183–3188.

26. Vilfan, A., and T. Duke. 2003. Two adaptation processes in auditory hair cells together can provide an active amplifier. *Biophys. J.* 85:191–203.

27. Wiggins, S. 1990. Introduction to applied nonlinear dynamical systems and chaos. Springer-Verlag, New York.

28. Aranson, I. S., and L. Kramer. 2002. The world of the complex Ginzburg-Landau equation. *Rev. Mod. Phys.* 74:99–143.

29. Rosenau, P., and A. Pikovsky. 2005. Phase compactons in chains of dispersively coupled oscillators. *Phys. Rev. Lett.* 94:174102.

30. Pikovsky, A., and P. Rosenau. 2006. Phase compactons. *Physica D.* 218:56–69.

31. Ermentrout, G. B., and N. Kopell. 1984. Frequency plateaus in a chain of weakly coupled oscillators. *SIAM J. Math. Anal.* 15:215–237.

32. Osipov, G. V., and M. M. Sushchik. 1998. Synchronized clusters and multistability in arrays of oscillators with different natural frequencies. *Phys. Rev. E Stat. Phys. Plasmas Fluids Relat. Interdiscip. Topics.* 58:7198–7207.

33. Ivanchenko, M. V., G. V. Osipov, V. D. Shalfeev, and J. Kurths. 2004. Synchronization of two non-scalar-coupled limit-cycle oscillators. *Physica D.* 189:8–30.

34. Köppl, C., and G. A. Manley. 1990. Peripheral auditory processing in the bobtail lizard *Tiliqua rugosa*. II. Tonotopic organization and innervation pattern of the basilar papilla. *J. Comp. Physiol.* [*A*]. 167:101–112.

35. Manley, G. A. 2004. Spontaneous otoacoustic emissions in monitor lizards. *Hear. Res.* 189:41–57.

36. Manley, G. A., C. Köppl, and B. M. Johnstone. 1990. Peripheral auditory processing in the bobtail lizard *Tiliqua rugosa*. I. Frequency tuning of auditory-nerve fibers. *J. Comp. Physiol.* [*A*]. 167:89–99.

37. Manley, G. A., G. K. Yates, C. Köppl, and B. M. Johnstone. 1990. Peripheral auditory processing in the bobtail lizard *Tiliqua rugosa*. IV. Phase locking of auditory-nerve fibers. *J. Comp. Physiol.* [*A*]. 167:129–138.

38. Shera, C. A. 2003. Mammalian spontaneous otoacoustic emissions are amplitude-stabilized cochlear standing waves. *J. Acoust. Soc. Am.* 114:244–262.